J Fluoresc (2010) 20:681–693
DOI 10.1007/s10895-010-0603-7

ORIGINAL PAPER

Novel Fluorophores as Building Blocks for Optical Probes for In Vivo Near Infrared Fluorescence (NIRF) Imaging

Jutta Pauli · Robert Brehm · Monika Spieles · Werner A. Kaiser · Ingrid Hilger · Ute Resch-Genger

Received: 10 August 2009 / Accepted: 29 January 2010 / Published online: 6 March 2010

Abstract Aiming at the identification of new fluorescent reporters for targeted optical probes, we assessed the application-relevant features of a novel asymmetric cyanine, DY-681, in comparison to the only clinically approved dye indocyanine green (ICG), the golden imaging standard Cy5.5, and the asymmetric cyanine DY-676 successfully exploited by us for the design of different contrast agents. This comparison included the analysis of the spectroscopic properties of the free fluorophores and their thermal stability in aqueous solution as well as their cytotoxic potential. In addition, the absorption and emission features of IgG-conjugated DY-681 were examined. The trimethine DY-681 exhibited spectral features closely resembling that of the pentamethine Cy5.5. Its high thermal stability in phosphate buffer saline (PBS) solution in conjunction with its low cytotoxicity, reaching similar values as determined for Cy5.5 and DY-676, renders this dye more attractive as ICG and, due to its improved fluorescence quantum yield in PBS, also superior to DY-676. Although in PBS, Cy5.5 was still more fluorescent, the fluorescence quantum yields (Φ_f) of DY-681 and Cy5.5 in PBS containing 5 mass-% bovine serum albumin (BSA) were comparable. Labeling experiments with DY-681 and the model antibody IgG revealed promisingly high Φ_f values of the bioconjugated dye.

Keywords Fluorescence · Cyanine dye · Cytotoxicity · Stability · In vivo fluorescence imaging · Quantum yield · Contrast agent · Optical probe

J. Pauli · R. Brehm · M. Spieles · U. Resch-Genger (✉)
BAM Federal Institute for Materials
Research and Testing, Division I.5,
Richard-Willstaetter-Str. 11,
12489 Berlin, Germany
e-mail: ute.resch@bam.de

W. A. Kaiser · I. Hilger (✉)
Institut für Diagnostische und Interventionelle Radiologie
des Klinikums der Friedrich-Schiller-Universität Jena (IDIR),
Forschungszentrum Lobeda,
Erlanger Allee 101,
07747 Jena, Germany
e-mail: ingrid.hilger@med.uni-jena.de

Introduction

Non-invasive and comparably inexpensive optical imaging techniques like near-infrared (NIR) fluorescence (NIRF) imaging have matured into important tools in biomedical research due to advances in instrumentation, label technologies, and probe design [1–10]. Typical applications are the non-invasive interrogation of molecular function in vivo in animal models for the detection of very early stages of diseases such as cancer, or monitoring of disease progression, and evaluating the effect of drugs [2, 5, 11–15]. At the core of NIRF imaging are NIR fluorophores that can be used either directly as non-targeted contrast agents or as fluorescent reporters in targeted probes [5, 10, 16]. Applicable dyes must absorb and emit within the diagnostic window between 650 and 900 nm [4, 5, 17] with a high intensity (high molar absorption coefficient (ε) at the excitation wavelength (λ_{ex}) and high fluorescence quantum yield (Φ_f)) under application-relevant conditions [5, 17–23] and should show a sufficient thermal and photochemical stability as well as adequate pharmacological properties. The latter include solubility in aqueous media, low non-specific binding, rapid clearance of the free dye or contrast agent, and low cytotoxicity [5]. Advantageous are also a high chemical reactivity of the labeling reagent for the covalent attachment to a biomarker-specific antibody,

antibody fragment or peptide for the synthesis of targeted optical probes [24] and, generally, a reasonable price. These requirements underline the importance of the availability of reliable ε and Φ_f data for NIR fluorophores in aqueous media and data on the cytotoxicity of these chromophores for the choice of fluorescent reporters for in vivo NIRF. However, many dye manufacturers provide only spectroscopic data in organic solvents and often, no fluorescence quantum yields, and especially cytotoxicity data are very rare [10, 25–28]. Similarly relevant for these applications are spectroscopic studies revealing the influence of serum proteins like bovine serum albumin (BSA) and the conjugation to antibodies or peptides typically used as biomarker-specific ligands in targeted probes [4, 6, 10, 17, 18, 29, 30].

Fluorescent dyes commonly used for NIRF are symmetric cyanines like the contrast agent indocyanine green (ICG), that does not contain reactive groups for biomolecule labeling, and, for the design of optical probes, the golden standard Cy5.5, that emits between 690 and 750 nm, and the longer wavelength fluorophores cypate and Cy7 fluorescing above 770 nm [5, 10, 16, 17]. Increasingly popular are also Alexa Fluor 680, IRDye 680, and IRDye 700DX as well as the red chromophores Alexa 750 and IRDye 800CW [17, 29]. At present, the only clinically approved NIR fluorescent dye is still ICG despite its considerable drawbacks [5, 10, 31–37]. This includes a low fluorescence quantum yield in aqueous solution [38] in conjunction with a very small Stokes shift, that both strongly hamper overall sensitivity. Other limitations are e.g. strong aggregation in aqueous media [39], strong binding to plasma proteins [40, 41], resulting in rapid elimination through the liver, and a low stability in aqueous media [40–42]. Moreover, despite its approval by the Food and Drug Administration (FDA), ICG has recently been reported to induce cytotoxic effect [26–28].

The search for novel fluorophores for NIRF recently encouraged us to exploit comparatively new and inexpensive asymmetric cyanine dyes of the DY family like DY-676 for the construction of targeted optical probes [43–45]. Although the signal-relevant features of DY-676 do not reach yet the spectroscopic properties of Cy5.5 [5, 15, 24], the NHS ester of DY-676 revealed an improved chemical reactivity in protein coupling reactions. This enabled e.g. labeling of the clinically used antibody fragment arcitumomab® directed against the biomarker carcinoembryonic antigen (CEA) that could not be achieved by us with Cy5.5 [44]. This result—in conjunction with the suitability of this high-affinity probe for NIRF imaging of CEA-expressing tumors—encouraged us to evaluate the spectroscopic properties, thermal stability, and cytotoxicity of different asymmetric cyanines in comparison to clinically approved ICG, the most prominent, yet comparatively expensive fluorophore Cy5.5, and our own workhorse DY-676. Special emphasis was dedicated to the novel NIR fluorophore DY-681, a promising potential substitute of Cy5.5.

Experimental

Materials

Indocyanine green (ICG) was purchased from Pulsion Medical Systems AG (Munich, Germany) and Cy5.5 from GE-Healthcare Amersham (Freiburg, Germany). DY-681 and DY-676 as well as DY-682 were provided by DYOMICS GmbH (Jena, Germany). The quantum yield standards oxazine 1 and IR 125 were obtained from Lambda Physik GmbH (Goettingen, Germany).

Phosphate buffered saline (PBS) was purchased from GIBCO Life Sciences (Paisley, Scotland) and bovine serum albumin (BSA; fraction V) from Merck KgaA (Darmstadt, Germany). For the cytotoxicity studies, we used the cell culture medium Dulbecco's Modified Eagle's Medium (DMEM) containing 10% (v/v) of heat inactivated fetal calf serum (FCS) from GIBCO BRL Life Technologies (Paisley, Scotland), microtiter plates from Greiner Bio-One GmbH (Frickenhausen, Germany), and an MTT assay (CellTiter96® Promega, Mannheim, Germany; see also "Cytotoxicity").

Dye-IgG conjugates of DY-676 and DY-681 were obtained by reacting IgG (from rabbit serum; Sigma-Aldrich Chemie GmbH; Steinheim, Germany) with the NHS esters of these fluorophores dissolved in dimethylformamide (DMF) following a protocol provided by the manufacturer DYOMICS using identical reaction conditions for both dyes (e.g. solvent, pH, temperature, reaction time). The labeling density or dye-to-protein (D/P) ratio was varied via the dye NHS ester-to-protein ratios (3:1, 6:1, 24:1) of the reaction mixture. The dye-IgG conjugates were purified chromatographically (column filled with Sephadex Medium, GE-Healthcare Amersham, Freiburg, Germany). The D/P ratios of the IgG conjugates were determined photometrically in PBS from the absorbances at 280 nm (corrected for dye contributions) and at the dye's longest wavelength absorption maximum following the typically employed formula from Mujumdar and Waggoner [46]. The molar absorption coefficients of the dyes and IgG were previously determined in PBS.

Methods

Spectroscopic studies

The absorption and the fluorescence spectra of DY-681, DY-676, Cy5.5, and ICG and the dye-IgG conjugates were determined in duplicate in PBS (pH 7.4) and in a solution

of 5 mass-% (w/v) BSA in PBS (PBS/BSA) at a dye (or species) concentration of 1×10^{-6} mol×L^{-1} at T=(25±1)°C. The absorption spectra were recorded on a CARY 5000 spectrometer (Varian Inc., Palo Alto, USA). The molar absorption coefficient ($\varepsilon\lambda_{(max)}$) of DY-681 at the dye's absorption maximum (λ_{max}) was obtained in PBS from three independent measurements of the absorption spectra of two different stock solutions (1×10^{-4} mol×L^{-1}, ethanol) for a fluorophore concentration of 1×10^{-6} mol×L^{-1}, yet not from a concentration series.

The fluorescence emission and fluorescence excitation spectra of the dyes were measured with a Spectronics Instruments 8100 (Spectronics Instruments, Westbury, USA) spectrofluorometer equipped with Glan Thompson polarizers and calibrated with physical transfer standards [47, 48]. The polarizers placed in the excitation and the emission channel were set to 0° and 54.7°, respectively [49]. Typically, the emission was excited at the blue vibronic shoulder of the longest wavelength absorption band using absorbances of 0.02–0.06 at the excitation wavelength to minimize fluorescence-reducing and -distorting inner filter effects and reabsorption.

All the fluorescence spectra were corrected for wavelenght- and polarization-dependent intrument-specific effects [47]. For the calculation of the BSA-binding induced shifts in absorption ($\Delta\nu_{abs}$) and the Stokes shift (ν_{St}), the absorption spectra on a wavenumber scale were obtained by multiplying the intensity of the measured absorption spectra with λ [50]. Spectrally corrected emission spectra on a wavenumber scale were obtained by multiplying the measured and spectrally corrected emission spectra by λ^2 [47, 50].

The fluorescence quantum yields of the fluorophores were determined in duplicate using dye and standard solutions freshly prepared by dilution of stock solutions (typical dye concentration of 1×10^{-4} mol×L^{-1}, solvent DMF, stored in the refrigerator at 4°C in the dark) using Eq. 1 (same excitation wavelength for sample and standard) [50].

$$\Phi_{f,x} = \Phi_{fs,t} \times \frac{F_x}{F_{st}} \times \frac{f_{st}(\lambda_{ex})}{f_x(\lambda_{ex})} \times \frac{n_x^2}{n_{st}^2} \quad (1)$$

$$f(\lambda_{ex}) = 1 - 10^{-A(\lambda_{ex})} = 1 - 10^{-\varepsilon(\lambda_{ex})cl} \quad (2)$$

Here, $f(\lambda_{ex})$ is the absorption factor at the excitation wavelength λ_{ex}. $f(\lambda_{ex})$, that is equivalent to formerly used absorptance [51], is nonlinearly linked to the absorbance A (λ_{ex}) via the Beer-Lambert law [47], see Eq. 2. F is the integral emission intensity, i.e., the area under the blank and spectrally corrected emission spectrum on a wavelength scale, and n the refractive index of the solvent(s) used. The subscripts x and st denote sample and standard (oxazine 1 in ethanol: $\Phi_{f,st}$=0.15; used as standard for DY-676, DY-681, and Cy5.5; IR 125 in DMSO: $\Phi_{f,st}$=0.22, employed as standard for ICG) [52]. No attempts were made to correct the measured absorption intensities for contributions from non-fluorescent species. In these cases (e.g. for DY-676 in PBS), the given Φ_f values equal only the fluorescence quantum yield of the solution and not that of the emitting species. Typical uncertainties of fluorescence quantum yield measurements as derived from previous experiments (relative standard deviations derived from six independent measurements) are ±2% (for Φ_f>0.5) [53] as well as ±5% (for Φ_f>0.4) and ±10% for weaker emitting dyes (for 0.2>Φ_f>0.02) and ±20% (for 0.02>Φ_f>0.005), respectively [54].

Thermal stability

The thermal stability of the NIR chromophores was determined from the absorption spectra of the dyes in PBS and in PBS/BSA (dye concentration 1×10^{-6} mol×L^{-1}) at 4°C and 37°C, respectively. For a diagnostically relevant time window of up to 72 h, the data were measured daily and then after 10 days (data not shown). For the data evaluation, the absorption intensities, taken from the main absorption maximum, were compared to the values obtained for the fresh solutions (0 h). To ensure that changes in absorption intensity correlate with changes in dye concentration and not with solvent evaporation, all the samples were controlled gravimetrically. Typical uncertainties (standard deviation from six replicates) of absorption measurements with transparent dilute solutions in this intensity range are ±2% [55].

Cytotoxicity

Dye cytotoxicity was determined for murine endothelial cells (SVEC4-10) in culture. The cells were grown in DMEM containing 10% (v/v) of heat inactivated FCS at 37°C, 10% CO_2, and a relative humidity of 95%. The cell cultures were routinely assessed for contamination with mycoplasma. For the cytotoxicity studies, the cells (1,000 cells per well) were seeded in microtiter plates and incubated with different concentrations of the DY dyes and ICG (concentrations: 0.5×10^{-6} M, 10×10^{-6} M, 100×10^{-6} M) as well as Cy5.5 (concentrations: 0.1×10^{-6} M, 10×10^{-6} M) for 24 and 72 h, respectively. The cell vitality was obtained from measurements of the activity of cellular dehydrogenase in dye-treated and non-treated cells after addition of 3-(4,5-dimethylthiazole-2-yl)-2,5-diphenylte trazoliumbromide (MTT, 20×10^{-6} L per well, 1.9 g/L). Living cells turned this tetrazolium salt into a blue formazan product, the concentration of which was deter-

mined photometrically from the absorption at 492 nm after an incubation time of 1 h using a microplate reader (Molecular Devices, CA, USA). The formazan concentration is directly proportional to the number of living cells in the respective cell culture. The cell vitality was expressed in relative numbers in relation to untreated controls. Values lower than 100% indicate cytotoxicity, higher values cell proliferation. The test was performed six times for each dye concentration.

Results

Spectroscopic properties

The chemical structures of the asymmetric cyanine DY-676 and DY-681 and the symmetric cyanines Cy5.5 and ICG are shown in Fig. 1, respectively. DY-676 and DY-681 carry the same indole end group equipped with two negatively charged sulfonate groups to promote water solubility, yet differ in the chemical nature of the aromatic benzopyrylium-type end group (acceptor strength, planarity, rigidity) and in the position of the attachment of the benzopyrylium group to the polymethine chain (DY-676: para attachment; DY-681: ortho attachment).

The spectroscopic properties of DY-676, DY-681, Cy5.5, and ICG are in summarized in Figs. 2, 3, 4 and 5 and in Table 1. The absorption and emission maxima of the trimethine DY-681 and the pentamethine Cy5.5 closely match in PBS and PBS/BSA and are slightly red-shifted compared to the trimethine DY-676. The absorption and emission spectra of the heptamethine ICG in PBS and PBS/BSA are red-shifted by approximately 100 nm.

As highlighted in Fig. 2, the absorption and emission spectra of Cy5.5, DY-676, and ICG in PBS display a clearly visible vibronic structure, as typically observed for cyanine dyes. The absorption and emission spectrum of DY-681, however, are broader and barely structured. The absorption and fluorescence excitation spectra of Cy5.5 and ICG in PBS match at the chosen dye concentration of 1×10^{-6} mol×L^{-1} (within the measurement uncertainty of the excitation correction). In contrast, the absorption and excitation spectra of DY-681 show small differences in the spectral region of the blurred vibronic shoulder around 620–660 nm. Similar mismatches occur for DY-676, with the size of these (concentration-dependent) deviations being more pronounced as the effects observed for DY-681.

As follows from Fig. 3, the shape of the normalized absorption spectra of DY-676 in PBS (Fig. 3, right) depends on dye concentration in the concentration range

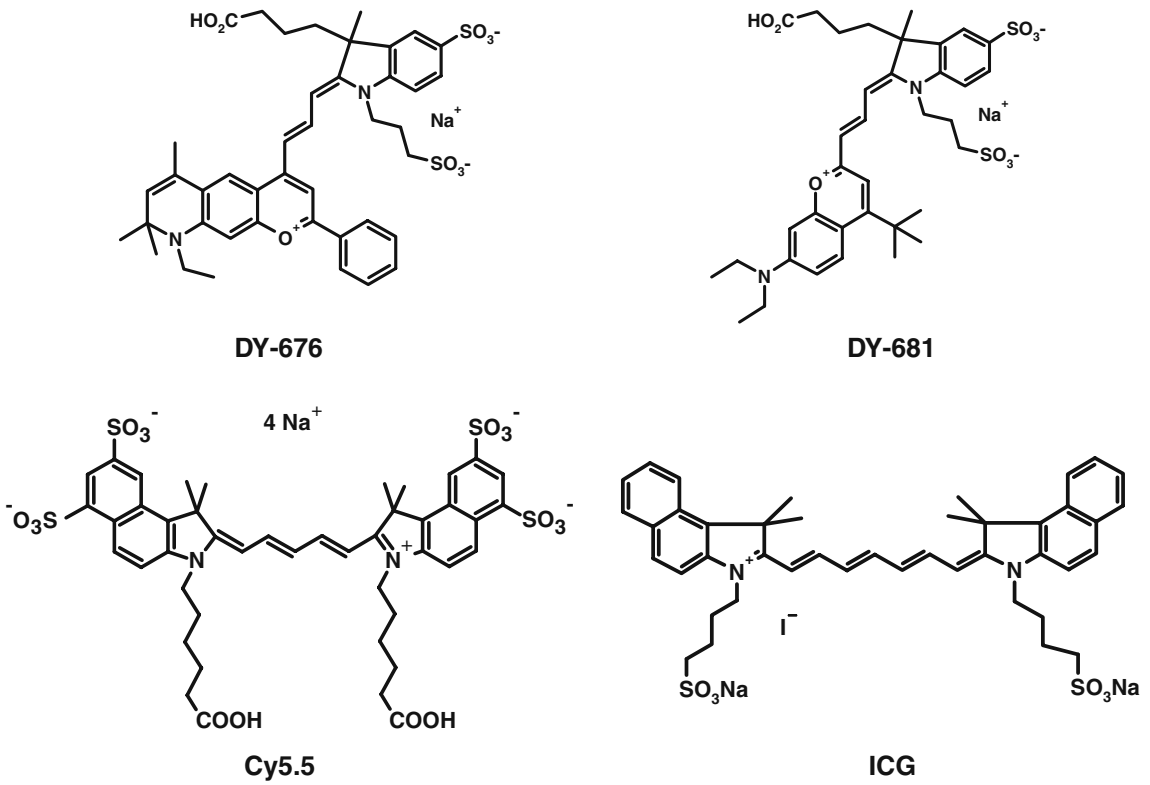

Fig. 1 Chemical structures of DY-676, DY-681, Cy5.5, and ICG

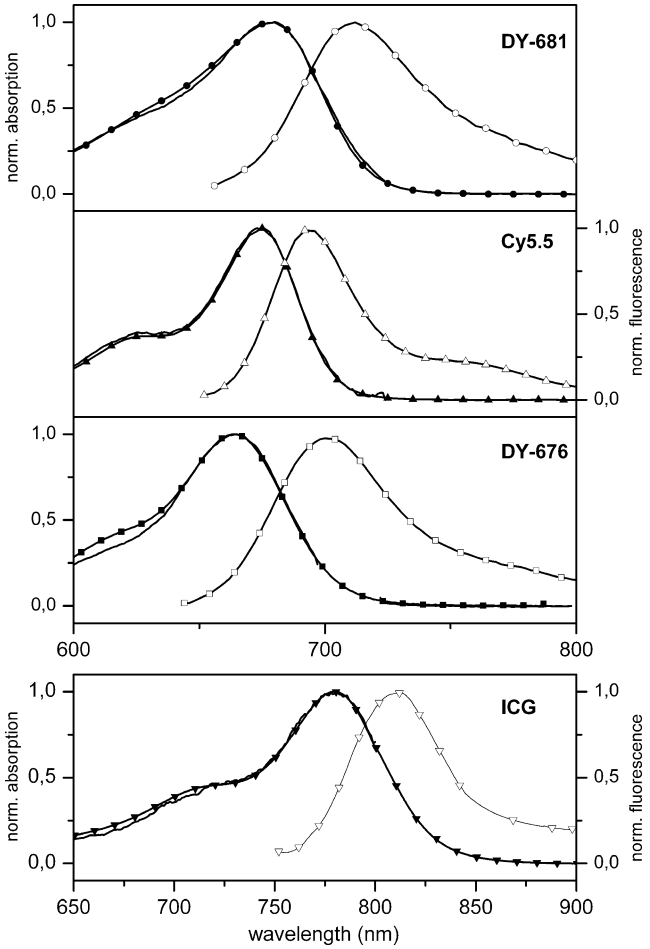

Fig. 2 Normalized absorption (*full symbols*), fluorescence excitation (*dashed lines*) and fluorescence emission (*open symbols*) spectra of DY-681 (*top panel*; λ_{em}=712 nm, λ_{ex}=629 nm) in comparison to Cy5.5 (*second panel*; λ_{em}=700 nm, λ_{ex}=615 nm), DY-676 (*third panel*; λ_{em}=710 nm, λ_{ex}=629 nm,) and ICG (*bottom panel*; λ_{em}= 806 nm, λ_{ex}=730 nm); solvent PBS, dye concentration of 1×10^{-6} mol×L^{-1}, T=25°C. The emission and excitation wavelengths used are given in brackets

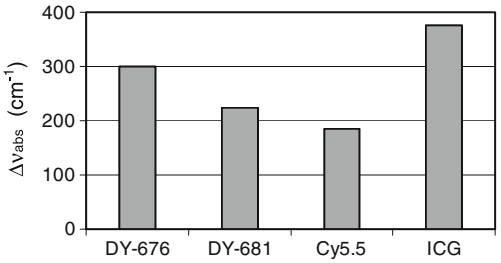

Fig. 4 BSA-induced spectral shift in the main absorption maximum $\Delta\nu_{abs}$ ($\Delta\nu_{abs}=\nu_{abs}(PBS)-\nu_{abs}$(PBS/BSA)) of DY-676, DY-681, Cy5.5, and ICG

of (2–0.05) × 10^{-6} mol L^{-1} (left, concentration-dependent intensity of the shoulder at ca. 620 nm and spectral broadening). Although the shape of the normalized absorption spectra of DY-681 (Fig. 3, left) is barely affected by dye concentration within the chosen concentration range, its molar absorption coefficient $\varepsilon(\lambda_{max})$, that was determined to 98,000 L mol^{-1} cm^{-1} (dye concentration of 1×10^{-6} M, T=25°C shows a slight concentration dependence. Cy5.5 does not display a detectable influence of dye concentration on its absorption in the concentration range of 2×10^{-6} M–0.05×10^{-6} mol×L^{-1}. There are literature reports on the concentration dependence of the absorption spectra of ICG [39, 56, 57], yet, we did not observe such effects here for our ICG. The emission spectra of DY-681, DY-676, Cy5.5, and ICG are always independent of dye concentration.

In the presence of BSA, DY-676, DY-681, Cy5.5, and ICG display a red shift in the absorption maximum ($\Delta\nu_{abs}$), see Fig. 4. The size of the BSA-induced spectral shift follows the order Cy5.5 < DY-681 < DY-676 < ICG. The spectral position of the emission band is only affected in the case of ICG, see Table 1. For both DY-676 and DY-681, also the width (Table 1, $FWHM_{abs}$) and spectral shape (Figs. 2

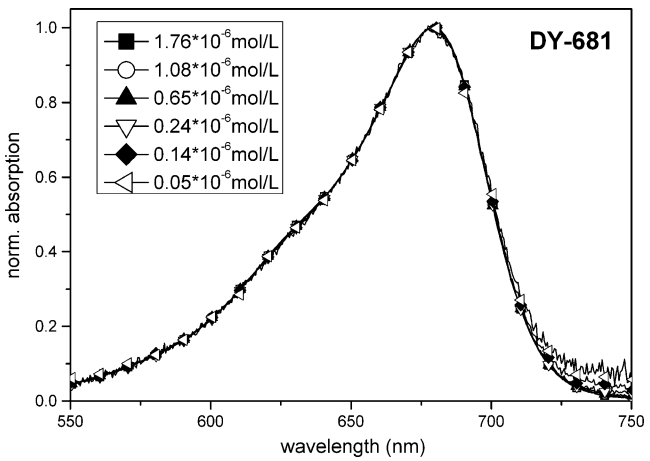

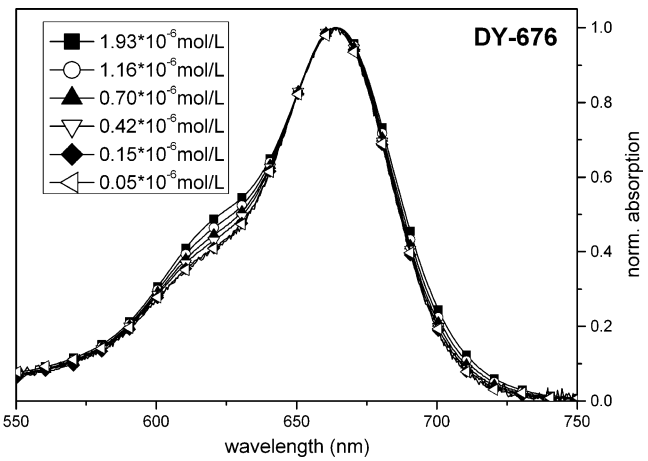

Fig. 3 Normalized absorption spectra of DY-681 (*left panel*; and DY-676 (*right panel*) in PBS as a function of dye concentration, concentration range $(2-0.05)\times10^{-6}$ mol L^{-1},T=25°C. The absorption spectra were normalized at the maximum of the absorption band at 678 nm (DY-681) and 664 nm (DY-676), respectively

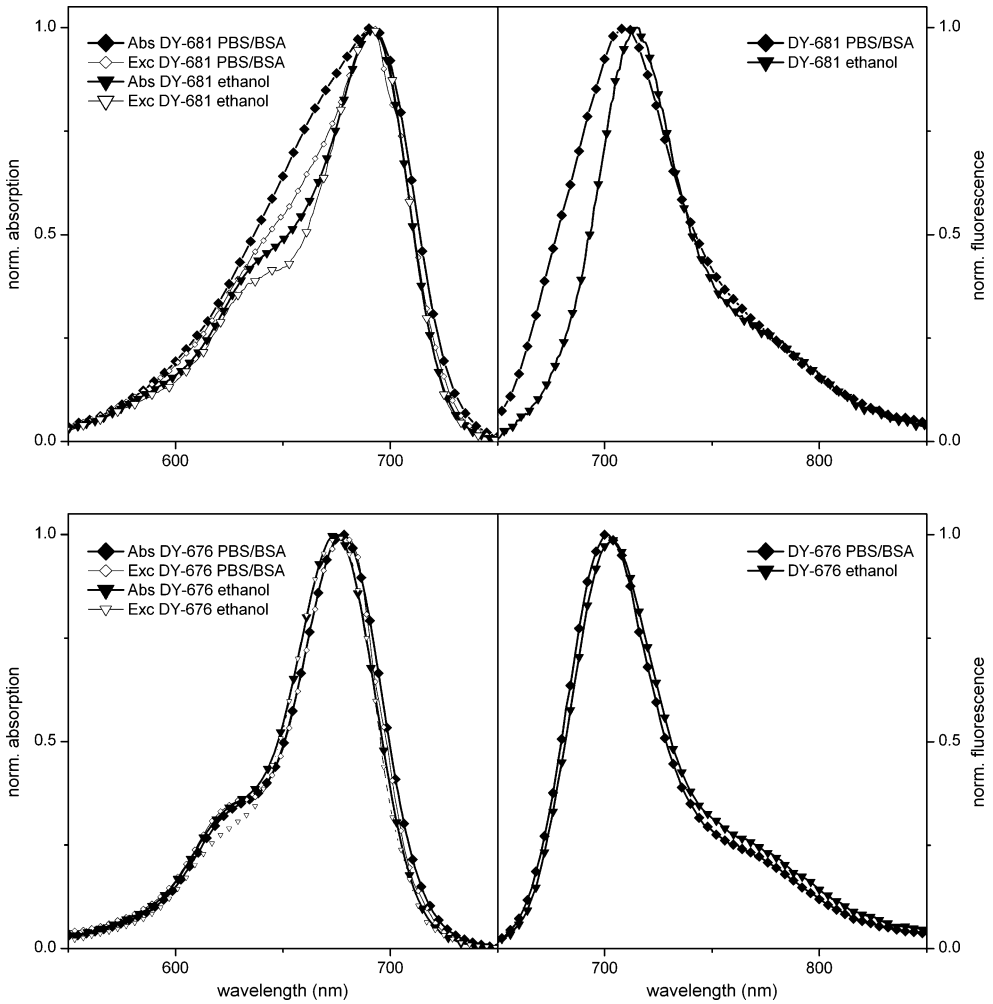

Fig. 5 Absorption and fluorescence excitation spectra (*left panel*) and fluorescence emission spectra (*right panel*) of DY-681 (*top*) in PBS/BSA (λ_{em}= 710 nm, λ_{ex}=629 nm) and in ethanol (λ_{em}=730 nm, λ_{ex}= 629 nm). For comparison, also the absorption, excitation, and emission spectra of DY-676 (*bottom*) in PBS/BSA (λ_{em}= 702 nm, λ_{ex}=629 nm), ethanol (λ_{em}=730 nm, λ_{ex}=629 nm) are included. The emission and excitation wavelengths used are given in brackets. The dye concentration was 1×10^{-6} mol L^{-1}, T=25°C

and 5) of the absorption band undergo considerable changes in the presence of BSA. In the case of DY-676, the presence of BSA reduces the intensity of the absorption shoulder at ca. 620 nm relative to the intensity of the absorption maximum and improves the spectral match between the absorption and fluorescence excitation spectrum. In contrast, for DY-681, also in PBS/BSA, the absorption and fluorescence excitation spectrum slightly deviate.

The different behavior of DY-676 and DY-681 in PBS and PBS/BSA encouraged us to study the absorption,

Table 1 Spectroscopic properties of the studied cyanines in PBS and PBS/BSA

Dye	Solvent	λ_{abs}[a]/nm	$FWHM_{abs}$[b]/cm^{-1}	λ_{em}[c]/nm	ν_{St}[d]/cm^{-1}	Φ_f[e]
DY-676	PBS	664	1,505	702	804	0.04
DY-676	BSA/PBS	678	1,009	702	504	0.31
DY-681	PBS	679	1,603	712	700	0.11
DY-681	BSA/PBS	690	1,627	710	397	0.40
Cy5.5	PBS	674	923	694	417	0.29
Cy5.5	BSA/PBS	683	1,062	694	396	0.43
ICG	PBS	780	1,011	810	514	0.04
ICG	BSA/PBS	807	973	822	258	0.08

Maximum of the main absorption band (λ_{abs})[a], full width at half-height of the (absorption) maximum ($FWHM_{abs}$)[b], maximum of the emission band (λ_{em})[c], Stokes shift (ν_{St}), i.e., energetic difference between the longest wavelength absorption band and the emission maximum ($\nu_{St}=\nu_{abs}-\nu_{em}$)[d], and fluorescence quantum yield (Φ_f)[e]. The dye concentration was 1×10^{-6} mol×L^{-1}, T=25°C

excitation, and emission spectra of both dyes also in the organic solvent ethanol (Fig. 5). Similarly as in PBS/BSA, the absorption (left) and emission (right) maxima of both DY-681 (Fig. 5, top) and DY-676 (Fig. 5, bottom) are red-shifted in ethanol in comparison to PBS (Table 1 and Fig. 2). DY-681 displays more structured absorption and fluorescence spectra in ethanol as compared to PBS and PBS/BSA, that are, nevertheless, still broader than the corresponding spectra obtained for DY-676 (Fig. 5, bottom). Also in ethanol, the absorption and fluorescence excitation spectra of DY-681 slightly differ. In the case of DY-676, such deviations result only in PBS (Fig. 2), whereas the corresponding spectra in PBS/BSA, and ethanol, (Fig. 5, bottom, left) match (taking the uncertainty of the excitation correction into account). Also, an enhanced intensity of the vibronic shoulder in the absorption spectrum of DY-676 was only found for PBS.

The fluorescence quantum yields of DY-676, DY-681, Cy5.5, and ICG in PBS and PBS/BSA are summarized in Table 1. In PBS, the Φ_f vales decrease in the order of Cy5.5 > DY-681 > DY-676 ≈ ICG. The presence of BSA yields a dye-specific fluorescence increase with the strongest fluorescence enhancement factor (FEF) of 7.8 resulting for DY-676 followed by DY-681 (FEF=3.6), ICG (FEF=2.0), and Cy5.5 (FEF=1.5). Although the Φ_f value of Cy5.5 exceeds that of DY-681 by a factor of 2.6 in PBS, in PBS/BSA, both dyes display almost identical fluorescence quantum yields.

Thermal stability

Figure 6 summarizes the results from a spectroscopic study of the thermal stability of the four dyes in PBS and PBS/BSA at 4°C and 37°C modeling the in vivo situation over 3 days.

The thermal stabilities of Cy5.5 and DY-681 as well as DY-676 are comparable and always very high. Only after 10 days in PBS at 37°C, the stability of DY-681 (0.49 a.u.) was found to be reduced as compared to Cy5.5 (0.90 a.u.) and DY-676 (0.59 a.u.). ICG shows always a lower stability (0.09 a.u.). Its thermal stability reveals a pronounced dependence on matrix, i.e., solvent and temperature, with a reduction in temperature and especially the presence of BSA resulting in an improved dye stability. Cy5.5, DY-681, and DY-676 display a similar trend, but much less pronounced.

Cytotoxicity

Table 2 highlights the cell vitality of an endothelial cell line (SVEC4-10) after incubation with defined concentrations of DY-676, DY-681, Cy5.5, and ICG determined with a dead-or-alive assay. Endothelial cells were used here because of the extensive contact of these cells with intravenously applied substances, thereby providing a good model for the in vivo NIRF situation in the vascular system. The concentration of the fluorophores are representative for in vivo experiments where fluorophore doses of approximately 55 nmol/kg body weight have been frequently given to small laboratory animals [12, 44].

Cy5.5 as well as DY-681 and DY-676 show very low cytotoxic effects. For an incubation time of 72 h at the maximum tested dye concentration of 10×10^{-6} M, the endothelial cell vitality is promisingly high for DY-681 and

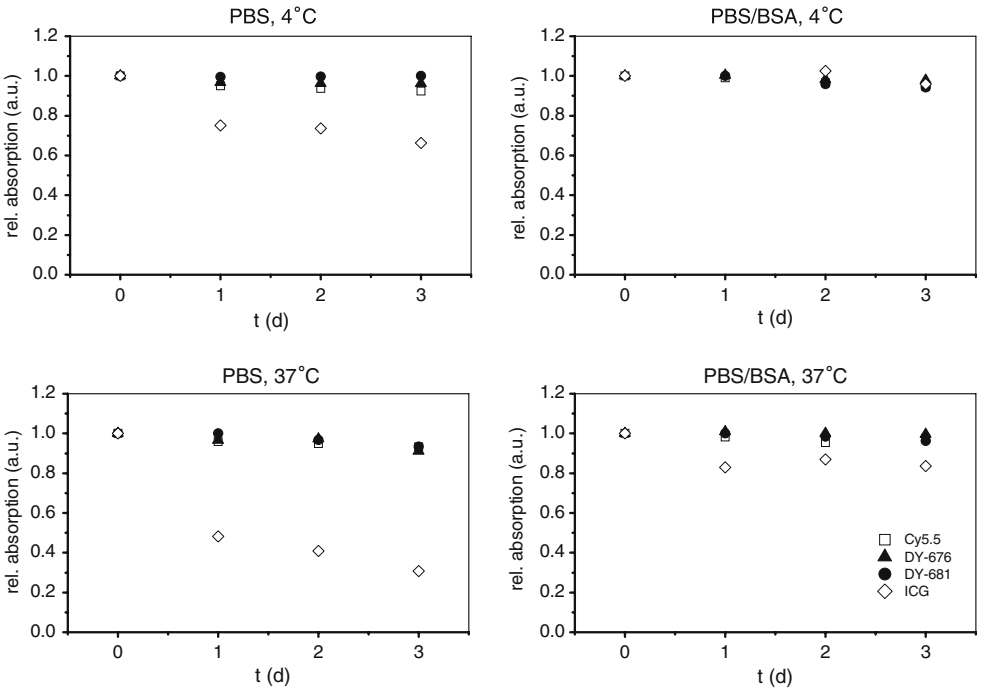

Fig. 6 Spectroscopically determined thermal stability of Cy5.5 (*open squares*) in PBS (*left panels*) and PBS/BSA (*right panels*) in comparison to DY-681 (*full circles*), DY-676 (*full triangles*), and ICG (*open rhombs*) at temperatures of 4°C (*top*) and 37°C (*bottom*), respectively, as a function of time provided in days (d) within a time window of 3 days. The dye concentration used was always 1×10^{-6} mol×L^{-1}. The absorption intensities were taken from the main absorption maximum and related to the values of the fresh solutions (0 h)

Table 2 Cytotoxicity of DY-681 in comparison to the cytotoxicity of DY-676, Cy5.5, and ICG determined for an endothelial (SVEC4-10) cell line after 24 h (top) and 72 h (bottom) of incubation with each dye

Concentration/ 10^{-6}mol×L^{-1}	DY-676	DY-681	Cy5.5	ICG
incubation time 24h				
0	100±1	100±5	100±1	100±5
0.1	n.d.[a]	n.d.	95±12	n.d.
0.5	n.d.	102±15	n.d.	110±15
10	96±2	92±8	95±11	100±13
incubation time 72 h				
0	100±2	100±5	100±2	100±2
0.1	n.d.[a]	n.d.	91±6	n.d.
0.5	90±15	99±17	n.d.	93±6
10	98±15	98±15	97±2	81±6

Cell cultures without any dye treatment exhibit a cell vitality of 100%

[a] not determined (n.d.)

DY-676 (cell vitality over 98%). In the case of Cy5.5, we found a comforting cell vitality of 97%. Astonishingly, the strongest cytotoxic effects resulted for clinically approved ICG (Table 2) with the vitality steadily decreasing with increasing dye concentration and eventually reaching a value of 81% at the maximum tested dye concentration of 10×10^{-6} M. A further increase in dye concentration to 100×10^{-6} M, that was only performed for DY-681, DY-676, and ICG to test these dyes under especially stringent conditions, yielded a high endothelial cell vitality of 96% for DY-681, 110% for DY-676, and only 60% for ICG, respectively.

Dye-antibody conjugates

First protein coupling reactions with DY-676 and DY-681 reveal a superior reactivity as compared to Cy5.5 resulting in efficient protein labeling and high labeling densities. The absorption spectra and the Φ_f-weighted emission spectra of the resulting DY-681-IgG conjugates in PBS are summarized in Fig. 7. We did not study Cy5.5-IgG conjugates here as these systems have been spectroscopically investigated already by Gruber et al. [58]

Conjugation of DY-681 to IgG results in a small red shift of the absorption and emission maximum in PBS by 8 nm and 2 nm, respectively. All the DY-681-IgG conjugates display an enhanced absorption at *ca*. 642 nm with the intensity of this peak—compared to the dye's main absorption band—increasing with increasing D/P ratio (Fig. 7, top). The spectral shape of the emission spectra of the DY-681-IgG conjugates is independent of D/P ratio, yet the fluorescence quantum yield and accordingly, the Φ_f-weighted emission spectra decrease with increasing labeling density (Fig. 7, bottom). Promisingly, with a fluorescence quantum yield of 0.07 in PBS found for a D/P ratio of about 1.5, the DY-681-IgG conjugates are considerably more emissive than the corresponding DY-676-IgG conjugates (Φ_f=0.02). In contrast to the nonconjugated dye, addition of BSA barely affects the spectral position and shape of the absorption and emission bands of the DY-681-IgG conjugates and their fluorescence quantum yields.

Discussion

Spectroscopic properties

As is evident from Figs. 2 and 5, DY-681. DY-676, Cy5.5, and ICG display cyanine-typical optical transitions delocalized over the whole π-conjugated system [36] in all the

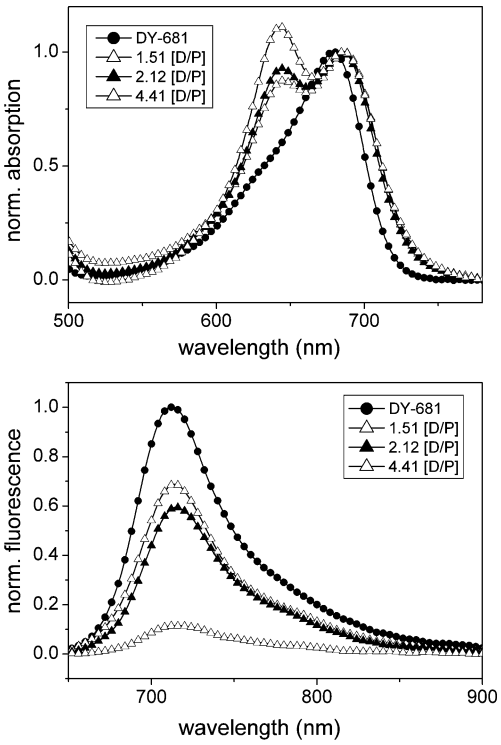

Fig. 7 Absorption spectra (*top*) and Φ_f-weighted emission spectra (*bottom*) of DY-681-IgG conjugates of various dye-to-protein (D/P) ratios in PBS in comparison to the corresponding spectra of nonconjugated DY-681 in PBS. The absorption spectra were normalized at the maximum of the absorption band at 687 nm, T=(25±1)°C

solvents studied. Intringuingly, with respect to its spectral properties, the trimethine dye DY-681 is a suitable substitute for the pentamethine Cy5.5. This underlines the great effective length of the benzopyrylium-type end group that is principally advantageous for the realization of cyanines with long wavelength absorption and emission bands with a minimum number of conjugated double bonds as a prerequisite for high fluorescence quantum yields [36, 56, 59, 60]. In addition, with a fluorescence quantum yield of 0.11 in PBS, DY-681 is considerably more emissive than DY-676 and ICG (Table 1). This is mainly ascribed to the enhanced hydrophilicity and reduced aggregation tendency of DY-681 (e.g. Fig. 3). Obviously, the replacement of the phenyl group of the *N*-bridged benzopyrylium entity of DY-676 by a smaller benzopyrylium moiety carrying a tert.-butyl and a diethylamino substituent in DY-681 is favorable for the minimization of typically fluorescence quenching dye-dye interactions, i.e., aggregation (H-dimer formation) [11, 36, 56, 58, 61–65]. The enhanced electron acceptor strength of this benzypyrylium entity accounts for the observed red shift of the absorption and emission bands of DY-681 compared to DY-676. At present, the most plausible explanation for the astonishingly broad absorption and emission bands of DY-681 in PBS as well as in PBS/BSA (Figs. 2 and 5), where dimerization is not very likely [66], is the formation of at least two more or less fluorescent conformers. This could also account for the mismatch of the absorption and fluorescence excitation spectra of DY-681 in these solvents as well as in ethanol (Figs. 2 and 5). The presence of fluorescent impurities can be excluded as revealed by HPLC analysis of DY-681 (only one peak observed). This assumption is further supported by first studies of the fluorescence decay behavior of DY-681 in these solvents. In contrast to e.g. monoexponentially decaying DY-676, DY-681 always reveals biexponential fluorescence decay kinetics (e.g. in PBS: τ_1=0.35 ns and τ_2=0.78 ns). For a complete understanding of the photophysics of DY-681, further time-resolved and temperature-dependent fluorescence studies are needed.

As follows from Table 1, although the fluorescence quantum yield of DY-681 in PBS is still lower than the Φ_f value found for Cy5.5, the fluorescence quantum yields of both dyes are comparable in PBS/BSA. This is encouraging for this type of asymmetric cyanine. The observed dye-dependence of the fluorophore-BSA interactions is attributed to differences in dye hydrophilicity and chromophore molecular structure (e.g. molecule size and steric effects) [67]. The generally observed BSA-induced fluorescence enhancement, that has been reported for other cyanine dyes as well [68, 69], is ascribed to a combination of different effects. This includes electrostatic and hydrophobic interactions between the fluorophores and the protein leading to a rigidization of the flexible dye molecules, thereby reducing rotations around single bonds in the polymethine chain and excited state cis-trans isomerization [36, 59, 60], as well as a better shielding of water molecules and a reduction in the polarity of the fluorophore local environment by the protein. The latter is reflected by the BSA-induced red shift of the absorption bands (Fig. 4 and Table 1). For example, the spectral position of the absorption maximum of DY-681 in PBS/BSA resembles the absorption maximum found in ethanol (Fig. 5, top, left), where this dye reveals a fluorescence quantum yield of 0.49. In the case of aggregating fluorophores like DY-676, the suppression of dye aggregation in PBS/BSA contributes additionally to the BSA-induced fluorescence increase as indicated by the matching absorption and fluorescence excitation spectra of DY-676 in this solvent (Fig. 5, bottom, left).

Thermal stability

The thermal stabilities of DY-681, Cy5.5, and DY-676 in PBS/BSA at 37°C, which approximates the in vivo situation by the presence of albumin and the use of body temperature, are encouraging with values of 0.96, 0.98 and 1.0 a.u., respectively, obtained after 3 days (Fig. 6). The stability of ICG is generally lower and is improved upon binding to BSA as previously reported [26, 27, 39]. The most important factor governing dye stability seems to be the shorter polymethine chains of the DY dyes and Cy5.5. The stability of DY-681, that is comparable to that of Cy5.5, is beneficial for the applicability of this dye as in vivo fluorescent agent.

Cytotoxicity

DY-681 generally exhibits distinctly lower cytotoxic effects on endothelial cells as ICG at high dye concentrations and a comparable cytotoxicity as Cy5.5. Contrary to ICG, even under more stringent conditions as used for Cy5.5, no cytotoxic effects could be detected for DY-681. The results found by us for ICG are in agreement with recent reports of a considerable cytotoxicity of ICG in vitro [27, 28, 70] and in vivo [27, 28]. The most probable mechanism for cell damage by ICG is an effect on mitochondrial enzyme activity leading to apoptosis [27], but other mechanisms could be involved as well. The observed lower cytotoxicty of DY-681, DY-676, and Cy5.5 is most likely related to the reduced lipophilicity/increased hydrophilicity of these fluorophores compared to ICG. A straightforward relationship between lipophilicity and cytotoxic effects has been revealed previously [71, 72]. Considering the fact that comparatively low fluorophore doses of approximately 55 nmol/kg body weight [12, 44] have been administrated systemically into mice, our cytotoxicity data indicate that

no distinct adversal local effects on endothelial cells emerging from the DY and Cy fluorophores are to be expected. Nevertheless, for potential applications as contrast agents in the clinical practice, extensive investigations related to the determination of lethal doses should be conducted.

Dye-antibody conjugates

The fluorescence properties of DY-681-IgG conjugates are more promising than those of the DY-676-IgG conjugates and other DY-676-antibody conjugates previously studied by us [44, 56]. For example, DY-676 conjugated to the antibody fragment arcitumomab directed against the biomarker CEA exhibited only a Φ_f value of 0.04, which was, however, sufficient for the highly selective and highly sensitive monitoring of tumors overexpressing CEA. Whether this is due to the excellent sensitivity of the imaging device used or at least partly related to the fact that the spectroscopic features of this targeted probe measured in solution differ from the properties of the probe bound to cancer cells overexpressing CEA is currently being studied by us.

Although being more emissive than conjugated DY-676, the fluorescence quantum yields of the DY-681-IgG conjugates in PBS are still lower than the Φ_f value of the free dye, even at a comparatively low D/P ratio of 1.5 (Fig. 7, bottom). Moreover, the diminution in fluorescence quantum yield corresponds with an increase of the absorption intensity of the blurred vibronic shoulder around 620 nm–660 nm (Fig. 7, top). Such a binding-induced reduction in emission, typically also in conjunction with the appearance of an enhanced absorption blue-shifted from the main absorption band, was reported for other bioanalytically relevant fluorescent labels including Cy5, Cy5.5, and the Alexa dyes [29, 30, 56, 58, 61, 62, 64, 65, 73, 74]. In the case of Cy5 for example, the fluorescence quantum yield of bioconjugated Cy5 drops to 0.10 for a D/P ratio of approximately 2 [75] and a 97% drop in fluorescence yield per Cy5 label has been described for the attachment of 6 dye molecules per IgG [58]. For Cy5.5, a similar behavior was reported [58]. We tentatively ascribe the IgG-binding-induced changes in the spectroscopic properties of DY-681 to nonfluorescent H-type dimers, the formation of which being indicated by the enhanced absorption around 620 nm–660 nm, and to fluorescence resonance energy transfer between chemically identical dye molecules on the same protein molecule (homo-FRET) [76, 77]. The non-emissive nature of these aggregates is underlined by the following results: First, the spectral shape of the emission of DY-681 is not affected upon conjugation to IgG and secondly, the deviations between the fluorescence excitation spectra of IgG-conjugated and nonconjugated DY-681 in the area of the enhanced absorption are increased. To derive the exact fluorescence quenching mechanism, further systematic studies are needed including fluorescence lifetime measurements and steady-state and time-resolved measurements of the emission anisotropy of these DY-681-IgG conjugates, that were beyond the scope of this article.

The comparison of the spectroscopic properties of DY-681, DY-676, Cy5.5, and ICG in PBS and in PBS/BSA and the results from the bioconjugation studies of DY-681 suggest that DY-681 is principally well suited as new fluorescent NIR label, yet its fluorescence quantum yield in aqueous solution and conjugated to biomolecules needs to be further enhanced. The most straightforward approach seems to be here the improvement of its hydrophilicity. This encouraged us to perform first spectroscopic studies with the only recently commercialized dye DY-682, shown in Fig. 8, that contains an additional sulfonate group.

DY-682 exhibits very similar absorption and emission spectra in PBS as DY-681, yet a promising increase in fluorescence quantum yield by a factor of approximately 2. In addition, first labeling experiments with this dye suggest that the higher Φ_f value of this fluorophore remains upon bioconjugation.

Conclusions

In summary, with DY-681 differing in substitution pattern of the benzopyrylium-type end group from previously studied DY-676, we identified an attractive and comparatively inexpensive fluorescent reporter for in vitro and in vivo fluorescence applications. This difference in substitution pattern seems to favorably reduce the dye's aggregation tendency. DY-681 exhibits comparatively red shifted absorption and emission bands, enhanced fluorescence quantum yields, a better thermal stability, and a clearly reduced cytotoxicity in comparison to clinically established

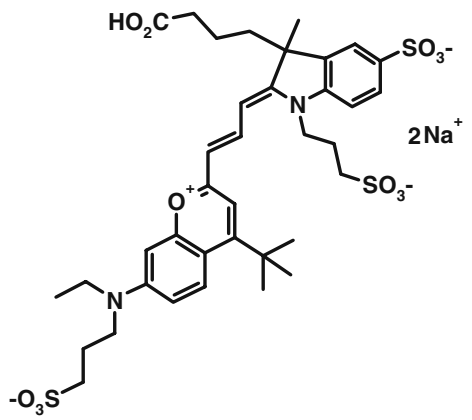

Fig. 8 Chemical structure of a new derivative of DY-681, DY-682, equipped with an additional sulfonate group at the benzopyrylium-type end group

ICG. Although its molar absorption coefficient and fluorescence quantum yield in aqueous solution are still lower than the values obtained for Cy5.5, the thermal stabilities and cytotoxities of both fluorophores are comparable and, in the presence of BSA, even the fluorescence quantum yields. A further improvement of the fluorescence quantum yield of DY-681 can be expected upon increasing its hydrophilicity as suggested by first studies of DY-682 containing an extra sulfonate group. These findings present an important advance toward new and comparatively less expensive tools of known stability and cytotoxicity for NIRF imaging. Moreover, these results underline the importance of known structure-property relationships and the availability of reliable spectroscopic data for aqueous solutions and for matrices modeling body fluid for the choice of optimum fluorophores.

Acknowledgements We are grateful to DYOMICS GmbH (Jena, Germany) for the generous supply of the dyes DY-676, DY-681, and DY-682. This work was partially supported by the Thüringer Aufbaubank. Furthermore, we thank Yvonne Heyne for assistance in the cytotoxicity studies and Franziska Hamann for the preparation of the IgG conjugates.

References

1. Bremer C, Ntziachristos V, Mahmood U, Tung CH, Weissleder R (2001) Advances in optical imaging. Radiologe 41:131–137
2. Weissleder R, Tung CH, Mahmood U, Bogdanov A (1999) In vivo imaging of tumors with protease-activated near infrared fluorescent probes. Nat Biotechnol 17:375–378
3. Weissleder R, Mahmood U (2001) Molecular imaging. Radiology 219:316–333
4. Ntziachristos V, Ripoll J, Wang LV, Weissleder R (2005) Looking and listening to light: the evolution of whole-body photonic imaging. Nat Biotechnol 23:313–320
5. Licha K (2002) Contrast agents for optical imaging. Top Curr Chem 222:1–29
6. Wagnières GA, Star WM, Wilson BC (1998) In vivo fluorescence spectroscopy and imaging for oncological applications. Photochem Photobiol 68:603–632
7. Achilefu S, Dorshow RB, Bugaj JE, Rajagopalan R (2000) Novel receptor-targeted fluorescent contrast agents for in vivo tumor imaging. Invest Radiol 35:479–485
8. Ranji M, Kanemoto S, Matsubara M, Grosso MA, Gorman JH III, Gorman RC, Jaggard DL, Chance B (2006) Fluorescence spectroscopy and imaging of myocardial apaptosis. J Biomed Opt 11:064036-1–064036-4
9. Mathejczyk J, Dullin C, Napp J, Resch-Genger U, Pauli J, Söling A, Tietze L-F, Kessler H, Alves F (2009) Functional and anatomical monitoring of glioblastoma xenografts in vivo by different imaging modalities. J Mol Imaging and Biology, submitted
10. Achilefu S (2004) Lighting up tumors with receptor-specific optical molecular probes. Technology in Cancer Research & Treatment 3:393–409
11. Hilderbrand SA, Weissleder R, Tung CH (2005) Monofunctional near-infrared fluorochromes for imaging applications. Bioconjug Chem 16:1275–1281
12. Hansch A, Frey O, Hilger I, Sauner D, Haas M, Schmidt D, Kurrat C, Gajda M, Malich A, Bräuer R, Kaiser WA (2004) Diagnosis of arthritis using near-infrared fluorochrome Cy5.5. Invest Radiol 39:626–632
13. Hilger I, Leistner Y, Berndt A, Fritsche C, Haas KM, Kosmehl H, Kaiser WA (2004) Near-infrared fluorescence imaging of HER-2 protein over-expression in tumour cells. Eur Radiol 14:1124–1129
14. Sevick-Muraca EM, Houston JP, Gurfinkel M (2002) Fluorescence-enhanced near infrared diagnostic imaging with contrast agents. Curr Op Biol 6:642–650
15. Bremer C, Ntziachristos V, Weitkamp B, Theilmeier G, Heindel W, Weissleder R (2005) Optical imaging of spontaneous breast tumors using protease sensing "smart" optical probes. Invest Radiol 40:321–327
16. Sutton EJ, Henning TD, Pichler BJ, Bremer C, Dahldrup-Link HE (2008) Cell tracking with optical imaging. Eur Radiol 18:2021–2031
17. Kovar JL, Simpson MA, Schutz-Geschwender A, Olive DM (2007) A systematic approach to the development agents for optical imaging of mouse of fluorescent contrast cancer models. Anal Biochem 367:1–12
18. Resch-Genger U, Grabolle M, Cavaliere-Jaricot S, Nitschke R, Nann T (2008) Quantum dots versus organic dyes as fluorescent labels. Nat Meth 5:763–775
19. Weissleder R, Ntziachristos V (2003) Shedding light onto live molecular targets. Nat Med 9:123–128
20. Ballou B, Lagerholm BC, Ernst LA, Bruchez MP, Waggoner AS (2004) Noninvasive imaging of quantum dots in mice. Bioconjug Chem 15:79–86
21. Patonay G, Antoine MD (1991) Near-infrared fluorogenic labels—new approach to an old problem. Anal Chem 63:A321–A326
22. Ballou B, Ernst LA, Waggoner AS (2005) Fluorescence imaging of tumors in vivo. Curr Med Chem 12:795–805
23. Adams KE, Ke SI, Kwon S, Liang F, Fan Z, Lu Y, Hirschi K, Mawad ME, Barry MA, Sevick-Muraca EM (2007) Comparison of visible and near-infrared wavelength-excitable fluorescent dyes for molecular imaging of cancer. J Biomed Opt 12:024017-1–024017-9
24. Holtke C, von Wallbrunn A, Kopka K, Schober O, Heindel W, Schafers M, Bremer C (2007) A fluorescent photoprobe for the imaging of endothelin receptors. Bioconjug Chem 18:685–694
25. Tong Z, Singh G, Rainbow AJ (2001) Extreme dark cytotoxicity of Nile Blue A in normal human fibroblasts. Photochem Photobiol 74:707–711
26. Ho JD, Tsai RJ, Chen SN, Chen HC (2003) Cytotoxicity of indocyanine green on retinal pigment epithelium. Implications for macular hole surgery. Arch Ophthalmol 121:1423–1429
27. Ikagawa H, Yoneda M, Iwaki M, Isogai Z, Tsujii K, Yamazaki R, Kamiya T, Zako M (2005) Chemical toxicity of indocyanine green damages retinal pigment epithelium. Invest Ophthalmol Vis Sci 46:2531–2539
28. Skrivanova K, Skorpikova J, Svihalek J, Mornstein V, Janisch R (2006) Photochemical properties of a potential photosensitiser indocyanine green in vitro. J Photochem Photobiol B Biol 85:150–154
29. Panchuk-Voloshina N, Haughland RP, Bishop-Stewart J, Bhalgal MK, Millard PJ, Mao F, Leung W-Y, Haughland RP (1999) Alexa dyes, a series of new fluorescent dyes that yield exceptionally bright, photostable conjugates. J Histochem Cytochem 47:1179–1188
30. Berlier JE, Rothe A, Buller G, Bradford J, Gray DR, Filanoski BJ, Telford WG, Yue S, Liu J, Cheung C-Y, Chang W, Hirsch JD, Beechem JM, Haughland RP, Haughland RP (2003) Quantitative comparison of long-wavelength Alexa Fluo dyes to Cy dyes: fluorescence of the dyes and their bioconjugates. J Histochem Cytochem 51:1699–1712

31. Bradley EC, Barr JW (1968) Determination of blood volume using indocyanine green (cardio-green) dye. Life Sci 7:1001–1007
32. Klocke FJ, Greene DG, Koberstein RC (1968) Indicator-dilution measurement of cardiac output with dissolved hydrogen. Circ Res 22:841–853
33. Benson RC, Kues HA (1978) Fluorescence properties of indocyanine green as related to angiography. Phys Med Biol 23:159–163
34. Leevy CM, Smith F, Longueville J (1967) Indocyanine green clearance as a test for hepatic function. Evaluation by dichromatic ear densitometry. JAMA 200:236–240
35. Galanzha EI, Shashkov EV, Tuchin VV, Zharov VP (2008) In vivo multispectral, multiparameter, photoacoustic lymph flow cytometry with natural cell focusing, label-free detection and multicolor nanoparticle probes. Cytometry A 73A:884–894
36. Stoyanov S (2001) Probes: dyes fluorescing in the NIR region. In: Raghavachari R (ed) Near-infrared applications in biotechnology. Marcel Dekker Inc., New York, pp 35–93
37. Golijanin D, Madeb RR, Singer E, Wood RW, Reeder JE, Dogra V, Wu G, Yao J, Joseph J, Erturk E, Messing EE (2007) Near infrared fluorescence (NIRF) for intraoperative imaging of renal cortical tumors using intravenous indocyanine green (ICG). J Endourol 21:A93–A94
38. Soper SA, Mattingly QL (1994) Steady-state and picosecond laser fluorescence studies of nonradiative pathways in tricarbocyanine dyes: Implications to the design of near-IR fluorochromes with high fluorescence efficiencies. J Am Chem Soc 116:3744–3752
39. Landsman MLJ, Kwant G, Mook GA, Zijlstra WG (1976) Light absorbing properties, stability and spectral stabilization of indocyanine green. J Appl Physiol 40:575–583
40. Muckle TJ (1976) Plasma protein binding of indocyanine green. Biochem Med 15:17–21
41. Moody ED, Viskari PJ, Colyer CL (1999) Non-covalent labeling of human serum albumin with indocyanine green: a study by capillary electrophoresis with diode laser-induced fluorescence detection. J Chromatogr B Biomed Sci Appl 729:55–64
42. Gathje J, Steuer R, Nicholes KR (1976) Stability studies on indocyanine green dye. J Appl Physiol 29:181–185
43. Lisy MR, Schüler E, Lehmann F, Czerney P, Kaiser WA, Hilger I (2006) Diagnosis of peritonitis using near-infrared optical imaging of in vivo labeled monocytes-macrophages. J Biomed Opt 11:064014-1–064014-9
44. Lisy MR, Goermar A, Thomas C, Pauli J, Resch-Genger U, Kaiser WA, Hilger I (2008) In vivo near infrared fluorescence imaging of carcinoembryonic antigen expressing tumor cells in mice. Radiology 247:779–787
45. Lisy MR, Hartung A, Lang C, Schuler D, Richter W, Reichenbach JR, Kaiser WA, Hilger I (2007) Fluorescent bacterial magnetic nanoparticles as bimodal contrast agents. Invest Radiol 42:235–241
46. Mujumdar RB, Ernst LA, Mujumdar SR, Waggoner AS (1989) Cyanine dye labeling reagents containing isothiocyanate groups. Cytometry 10:11–19
47. Resch-Genger U, Pfeifer D, Monte C, Pilz W, Hoffmann A, Spieles M, Rurack K, Hollandt J, Taubert D, Schönenberger B, Nording P (2005) Traceability in fluorometry: part II. Spectral fluorescence standards. J Fluoresc 15:315–336
48. Pfeifer D, Hoffmann K, Hoffmann A, Monte C, Resch-Genger U (2006) The Calibration Kit Spectral Fluorescence Standards—A simple and certified tool for the standardization of the spectral characteristics of fluorescence instruments. J Fluoresc 16:581–587
49. Mielenz KD, Cehelnik ED, McKenzie RL (1976) Elimination of polarization bias in fluorescence intensity Measurements. J Chem Phys 64:370–374
50. Lakowicz JR (2006) Principles of fluorescence spectroscopy, 3rd edn. Springer Science+Business Media, New York
51. Braslavsky SE (2007) Glossary of terms used in photochemistry. Pure Appl Chem 79:293–465
52. Sens R, Drexhage KH (1981) Fluorescence quantum yield of oxazine and carbazine laser dyes. J Lumin 24/25:709–712
53. Grabolle M, Spieles M, Lesnyak V, Gaponik N, Eychmüller A, Resch-Genger U (2009) Determination of the fluorescence quantum yield of quantum dots: Suitable procedures and achievable uncertainties. Anal Chem 81:6285–6294
54. Rurack K, Bricks JL, Schulz B, Maus M, Reck G, Resch-Genger U (2000) Substituted 1, 5-diphenyl-3-benzothiazol-2-yl-2-pyrazolines: synthesis, X-ray structure, photophysics, and cation complexation properties. J Phys Chem A 104:6171–6188
55. Resch-Genger U, Hoffmann K, Nietfeld W, Engel A, Neukammer J, Nitschke R, Ebert B, Macdonald R (2005) How to improve quality assurance in fluorometry: fluorescence-inherent sources of error and suited fluorescence standards. J Fluoresc 15:337–362
56. Pauli J, Vag T, Haag R, Spieles M, Wenzel M, Kaiser WA, Resch-Genger U, Hilger I (2009) An in vitro characterization study of new near infrared dyes for molecular imaging. Eur J Med Chem 44:3496–3503
57. Mauerer M, Penzkofer A, Zweck J (1998) Dimerization. J-aggregation and J-disaggregation dynamics of indocyanine green in heavy water. J Photochem Photobiol B Biol 47:68–73
58. Gruber HJ, Hahn CD, Kada G, Riener CK, Harms GS, Ahrer W, Dax TG, Knaus HG (2000) Anomalous fluorescence enhancement of Cy3 and Cy3.5 versus anomalous fluorescence loss of Cy5 and Cy7 upon covalent linking to IgG and noncovalent binding to avidin. Bioconjug Chem 11:696–704
59. Mishra A, Behera RK, Behera PK, Mishra BK, Behera GB (2001) Cyanines during the 1990s: a review. Chem Rev 100:1973–2011
60. Rettig W, Rurack K, Sczepan M (2000) From cyanines to styryl bases—Photophysical properties, photochemical mechanism, and cation sensing abilities of charged and neutral polymethinic dyes. In: Valeur B, Brochon JC (eds) Methods and applications of fluorescence spectroscopy. Springer, Berlin, pp 125–227
61. Schobel U, Egelhaaf H-J, Brecht A, Oelkrug D, Gauglitz G (1999) New donor-acceptor pair for fluorescent immunoassays by energy transfer. Bioconjug Chem 10:1107–1114
62. Schobel U, Egelhaaf H-J, Fröhlich D, Brecht A, Oelkrug D, Gauglitz G (2000) Mechanism of fluorescence quenching in donor-acceptor labeled antibody conjugates. J Fluoresc 10:147–154
63. Ballou B, Fisher GW, Waggoner AS, Farkas DL, Reiland JM, Jaffe R, Mujumdar RB, Mujumdar SR, Hakala TR (1995) Tumor labeling in-vivo using cyanine-conjugated monoclonal antibodies. Cancer Immunol Immunother 41:257–263
64. Ogawa M, Kosaka N, Choyke PL, Kobayashi H (2009) H-Type dimer formation of fluorophores: a mechanism for activatable, in vivo optical molecular imaging. Cancer Res 69:1268–1272
65. West W, Pearce S (1965) The dimeric state of cyanine dyes. J Phys Chem 69:1894–1903
66. Philip R, Penzkofer A, Bäumler W, Szeimies RM, Abels C (1996) Absorption and fluorescence investigation of indocyanine green. J Photochem Photobiol A Chem 96:137–148
67. Ahn YH, Lee JS, Chang YT (2008) Selective human serum albumin sensor from the screening of a fluorescent rosamine library. J Com Chem 10:376–380
68. Kessler MA, Wolfbeis OS (1992) Laser-induced fluorescence determination of albumin using long wavelength absorbing molecular probes. Anal Biochem 20:254–259
69. Antoine MD, Devanathan S, Patonay G (1991) Determination of hydrophobicity of albumins and other proteins using a near-infrared probe. Spectrochim Acta 47A:501–508
70. Enaida H, Sakamoto T, Hisatomi T, Goto Y, Ishibashi T (2002) Morphological and functional damage of the retina caused by intravitreous indocyanine green in rat eyes. Graefes Arch Clin Exp Ophthalmol 240:209–213
71. Riefke B, Licha K, Semmler W (1997) Contrast media for optical mammography. Radiologe 37:749–755

72. Cascorbi I, Foret M (1991) Interaction of xenobiotics on the glucose-transport system and the Na+/K(+)-ATPase of human skin fibroblasts. Environ Saf 21:38–46
73. Luschtinetz F, Dosche C, Kumke MU (2009) Influence of streptavidin on the absorption and fluorescence properties of cyanine dyes. Bioconjug Chem 20:576–582
74. Cox WG, Beaudet MP, Agnew JY, Ruth JL (2004) Possible sources of dye-related signal correlation bias in two-color DNA microarray assays. Anal Biochem 331:243–254
75. Povrozin YA, Kolosova OS, Obukhova OM, Tatarets AL, Sidorov VI, Terpetschnig EA, Patsenker LD (2009) Seta-633-A NIR fluorescence lifetime label for low-molecular-weight analytes. Bioconjug Chem 20:1807–1812
76. Demchenko AP (2005) Optimization of fluorescence response in the design of molecular biosensors. Anal Biochem 343:1–22
77. Runnels LW, Scarlata SF (1995) Theory and application of fluorescence homotransfer to melittin oligomerization. Biophys J 69:1569–1583